R. F. Broom R. B. Laibowitz Th. O. Mohr W. Walter

Fabrication and Properties of Niobium Josephson Tunnel Junctions

The fabrication of thin-film Nb tunnel junctions is described. The main emphasis is on improvement of the tunneling characteristics through studies of the conditions influencing the formation of the tunnel barrier. In situ ellipsometric measurements have been made during growth of the tunnel oxide on the base electrode of the junctions in an rf plasma. The results are compared with electrical measurements on completed junctions. Two additional processes are found to have an important influence on the junction characteristics: precleaning of the base electrode in an Ar plasma before oxidation and a further treatment of the grown oxide in a low-voltage, high-pressure plasma. At the present time, the most effective gas for this process is N_2 . Data on annealing, storage effects, and thermal cycling are discussed. Finally, the results obtained on arrays of 80 two-junction interferometers are found to be rather encouraging for the design and construction of high-density memory arrays.

Introduction

Niobium is an attractive element for the electrodes of Josephson tunnel junctions for several reasons. In comparison to other elemental superconductors such as In, Sn, and Pb, it is harder, is more stable, and has a much greater tensile strength. As a result, thin films deposited on insulating substrates are able to withstand the strains induced by differential thermal contraction on cooling to 4 K without rupture or plastic flow. Resistance to damage by repeated thermal cycling is an important consideration for all applications, in particular for cryogenic computer circuits [1, 2].

Niobium has several oxides, among which NbO, NbO₂, and Nb₂O₅ have been identified [3, 4]. The latter can be grown to a precisely controlled thickness by anodic oxidation. In this form it is stable and free from defects such as pinholes, and is therefore very suitable for electrical isolation and protection of the underlying metal against chemical attack. For complex structures with several layers of insulation and metallization, the use of such a native oxide considerably improves the isolation integrity.

Among the elemental superconductors, Nb has the highest superconducting transition temperature: T_c = 9.2 K. Thus, junctions can be operated in liquid He at atmospheric pressure where the temperature is sufficiently low (4.2 K) that small temperature fluctuations have a negligible effect on junction parameters such as the gap voltage $2\Delta/e$ and the dc Josephson current i_1 . On the other hand, Nb is difficult to evaporate, requiring high temperatures (≈3000 K) and nearly ultrahigh-vacuum (uhv) conditions. The latter is especially important because of the propensity of Nb to getter gaseous impurities, particularly O2, which can lead to degradation of the films' superconducting properties [5]. Thin oxides (2-4 nm) suitable for tunneling have a relatively poorly defined structure, as evidenced by nonideal current-voltage (I-V) characteristics in the Bardeen-Cooper-Schrieffer (BCS) sense. Finally, the dielectric constant ϵ of the oxide is approximately three times higher than that of PbO or In₂O₃. For some applications this can be a disadvantage because of the reduction in switching speed or decreased voltage between junction resonances.

Copyright 1980 by International Business Machines Corporation. Copying is permitted without payment of royalty provided that (1) each reproduction is done without alteration and (2) the *Journal* reference and IBM copyright notice are included on the first page. The title and abstract may be used without further permission in computer-based and other information-service systems. Permission to *republish* other excerpts should be obtained from the Editor.

However, the good features of Nb are sufficiently rewarding to justify a serious effort to overcome the disadvantages. Thin films of Nb having a T_c close to the bulk value and resistance ratios greater than three can be made by sputtering [6] and by evaporation using e-beam heating [7]. As long as the native oxide of Nb is used to form the tunneling barrier we cannot expect to greatly modify ϵ ; however, in situations where the high capacitance presents problems, some measures are available to minimize the effect, e.g., increasing the Josephson current density j_1 or making a corresponding reduction in junction area.

The most important problem at present is attainment of reproducible and good *I-V* characteristics, *i.e.*, behavior as close as possible to the "ideal" BCS predictions. This goal is the principal motivation for the studies described in this paper.

The first reported tunneling experiments on Nb were made by Sherrill and Edwards [8], using bulk material oxidized in air with evaporated Pb counter electrodes. Shortly afterwards, Townsend and Sutton performed tunneling experiments with Pb [9] and Sn [10] counter electrodes. The rather good tunnel characteristics yielded a gap voltage $2\Delta(0)/e = 3.05$ mV and $2\Delta(0)/kT_c = 3.84$ [9] (close to presently accepted values [11]).

The first measurements on evaporated Nb films were reported by Giaever in 1962 [12]. Since then there have been many publications in which Pb [6, 11, 13-20], In [11, 21-24]), and Sn [25, 26] have been used as counter electrodes. In most cases the Nb films were deposited by sputtering [6, 13-20]; however, Nb foil [25, 26] and single-crystal Nb [11, 21-24] have also been used. A variety of methods have been used for growing tunnel oxides, most frequently thermal oxidation in air or dry O, [11-13, 15-16, 19-24]. Gas discharges, either dc [6, 14, 17] or rf [7] have also been used successfully, although the oxidation in these cases proceeds much more rapidly (suitable tunnel resistances are obtained in ≈1 min, as compared with ≈1 h for thermal oxidation). Barriers composed of Ge and InSb have been studied by Keller and Nordman [18].

At present there is not very plentiful data on all-Nb tunnel junctions; Laibowitz and Mayadas [27] have described junctions having the barrier formed by oxidized Al. The first all-Nb junctions having a tunnel barrier composed of native Nb oxide were reported by Laibowitz and Cuomo [24]; the oxide was formed by wet anodization. However, they found rather poor I-V characteristics in comparison with those they obtained with Pb, In, or Sn counter electrodes. Hawkins and Clarke [28] found that a thin film of Cu (\approx 0.8 nm) deposited on top of a thermally

grown oxide before deposition of the Nb counter electrode was necessary to prevent short circuits. In contrast, tunnel oxides formed by rf plasma oxidation [7] do not require this intermediate film and very rarely yield shorts. In all cases, however, the *I-V* characteristics with Nb counter electrodes deviated more strongly from the BCS dependence than the best examples having Pb, Sn, or In counter electrodes [7, 29].

Experimental details

• Junction fabrication

Fabrication of Josephson junctions requires three basic processing techniques: patterning of the electrodes and lines, deposition of superconducting material, and barrier preparation. The Josephson devices were placed on Si wafers because these offer readily available clean, polished, and thermally oxidized surfaces. These wafers can also be easily sectioned (diced) into chips as desired. The base- and counter-electrode patterns were obtained by the standard photoresist lift-off technique (®AZ-1350 [30]). Because of high internal strain in the Nb films, the resist layer had to be kept as thin as possible to avoid poor edge definition of the patterned films. In addition, resist adhesion to the substrate required improvement to prevent peeling before film deposition was completed. To date, the best solution has been a 5-min exposure of the wafer to an rf argon plasma of ≈1 Pa and 400 V prior to resist spinning. (All rf voltages given in this paper are peak-topeak voltages measured at the cathode.) The deposition of Nb from an e-gun and barrier growth in an oxidizing rf plasma ambient were performed in the vacuum system shown schematically in Fig. 1.

Five wafers mounted on the cathode could be processed individually, or simultaneously in one pumpdown. They were cleaned for 10 min in an rf Ar plasma (as above) before starting the base-electrode deposition. Typical conditions for Nb evaporation were a pressure below $\approx 10^{-5} \, \text{Pa}$ ($\leq 10^{-6} \, \text{Pa}$ at start), a substrate temperature of 40°C for the deposition of both electrodes, and a Nb deposition rate of 1-4 nm/s. Usual thicknesses for the electrodes were 110-130 nm for the base electrode and 220-300 nm for the counter electrode. Junctions were fabricated with dimensions ranging from $2 \times 2 \mu \text{m}^2$ to $30 \times 20 \mu \text{m}^2$ and both cross-line and inline geometries were realized. A scanning electron micrograph of a $10 \times 4.6 \mu m^2$ Nb junction is shown in Fig. 2. The smooth well-defined films and film edges are typical of all-Nb junctions.

The fabrication step with most influence on junction properties is formation of the tunneling barrier. We adopted the technique of rf plasma oxidation in order to

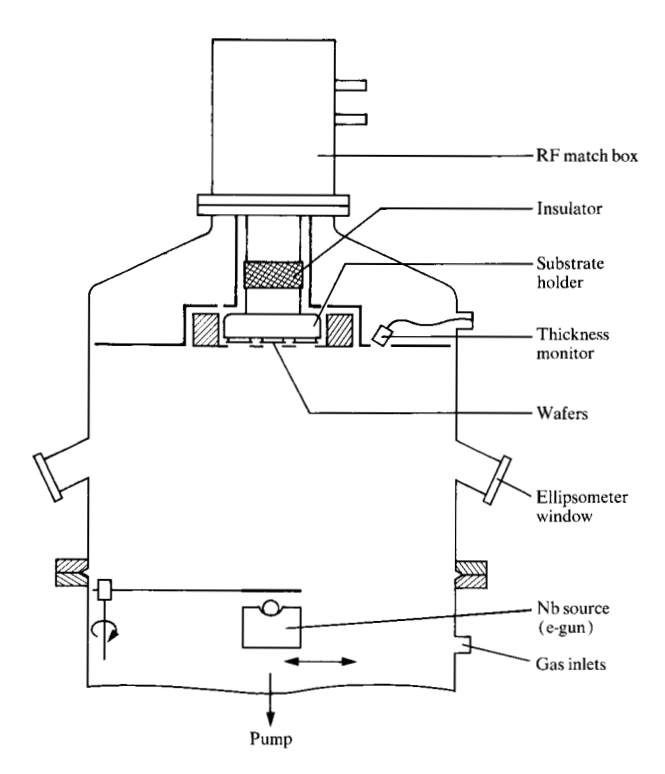


Figure 1 Schematic diagram of the rf oxidation system.

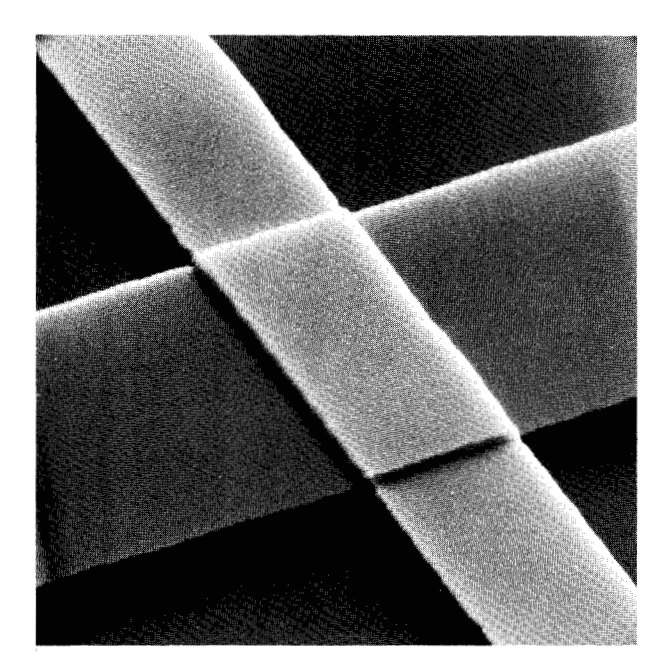


Figure 2 SEM photograph of an all-Nb junction. In this example the base- and counter-electrode thicknesses are 115 and 250 nm, respectively.

grow the barrier as a thin niobium oxide layer out of the base-electrode material. This technique has been successful in the fabrication of Pb and Pb-alloy Josephson junctions [31, 32]. The two basic processes taking place in the rf plasma are oxide growth and sputter etching. If both proceed at an equal rate, an equilibrium oxide thickness is reached. In the vacuum system the rf-plasma discharge occurs in the space between the cathode and the grounded bell jar and base plate. Discharge conditions are easily varied by changing gas pressure, composition, and rf power or voltage. This variability was very valuable in our investigations because the tunneling characteristics were found to be strongly influenced by both the oxidation conditions and any plasma treatment of the surface before (pre-cleaning) or after (post-treatment) formation of the tunneling oxide. The various gases used were O_a , Ar, and N₂. Pure Ar and N₂ were used to clean the baseelectrode layer and to change surface conditions of the asgrown barrier layer. A mixture of O2 with Ar or N2 was used to grow the barrier. Typical data and dependencies are given later.

Conventional equipment was used for controlling and monitoring gas pressure, gas composition, substrate temperature, rf power and voltage, deposition rate, and film thickness. In addition, an ellipsometer was mounted directly to the vacuum system to determine the polarization state of monochromatic light ($\lambda = 546.1$ nm) reflected from the sample at 70° , and to calculate the thickness and refractive index of the barrier layer according to the evaluation procedure described by F. L. McCrackin [32]. The rf glow discharge was switched off during the measurement to avoid stray light. This interruption had no detectable influence on barrier growth.

Electrical measurements

Electrical measurements were made with the junctions immersed in liquid He at 4.2 K. Samples of the cross-line geometry had current and potential contacts as shown in Fig. 3; however, the small in-line junctions had only a single contact pad for the counter electrode and in this case, a superconducting contact between the pad and the Pb-coated springs of the sample holder was necessary to avoid distortion of the true characteristic by contact resistance.

In order to make quantitative comparisons between different fabrication conditions, it is necessary to have a means of describing critical regions of the characteristic by easily definable parameters. To this end the measurements must be accurate and reproducible. The method adopted here was to automatically record the junction data (point by point) with a Research Device Coupler [33]. The accuracy and reproducibility of the measuring

system is better than 1%. An I-V plot normalized to I_0 , the maximum current at 4 mV, is shown in Fig. 4. The minimum number of points required to reconstruct the essential parts of the original characteristic was found to be sixteen.

The basic data of such plots are then used to calculate a number of parameters useful in comparing small changes not easily distinguishable in the *I-V* curves [34]. This procedure has the advantage of yielding some basis for comparison between Nb and Pb-alloy junctions. The parameters are as follows:

- Superconducting gap voltage $2\Delta/e = (1/2)[V(0.4 I_0) + V(0.6 I_0)];$
- Normal-state tunnel resistance $R_{nn} = 4 \text{ mV/}I_0$;
- R_i , the resistance at 2 mV;
- Maximum dc Josephson current $i_1 = 1.68 [(1/R_{nn}) (1/R_i)];$
- $V_{\rm m} = R_{\rm i}i_{\rm r}$; and
- Josephson current density $j_1 = i_1/\ell W$ ($\ell = \text{junction length}$, W = junction width).

The factor 1.68 in the equation for i_1 is somewhat arbitrary but represents an approximate upper limit to the experimentally observed Josephson current. It is, however, considerably lower than that obtained from the Ambegao-kar and Baratoff relation [35],

$$i_{1} = \frac{\pi}{2} \frac{\Delta(T)}{e} \frac{1}{R_{nn}} \tanh \frac{\Delta(T)}{2kT} ,$$

which yields $i_1 \approx 2.15/R_{\rm nn}$ for $\Delta/e = 1.42$ mV and T = 4.2 K, and ignores the strong coupling factor (which in any case is not expected to be significantly less than 0.9 for Nb [36]). In judging junction quality the most useful parameter is $V_{\rm m}$ because it yields a measure of the non-BCS tunnel current.

Results and discussion

• Ellipsometry and tunnel oxide growth

The tunnel barrier was grown as a thin niobium oxide layer from the Nb base-electrode material. The oxides were fabricated in a controlled rf process (130 V) using 5 Pa of Ar/O_2 mixtures with 0.5-4.0 vol% O_2 . Figure 5 gives the oxide thickness t_{ox} as a function of the oxidation time. The Nb films for these studies covered the whole wafer, but junctions were prepared simultaneously on neighboring wafers. The first ellipsometric reading was taken from the as-deposited or rf-cleaned (Ar) Nb surface, and resulted in an index of refraction $(n = n' - i\kappa)$ of 2.85 and a κ of 3.39 for Nb, which compares reasonably well with published data [37, 38].

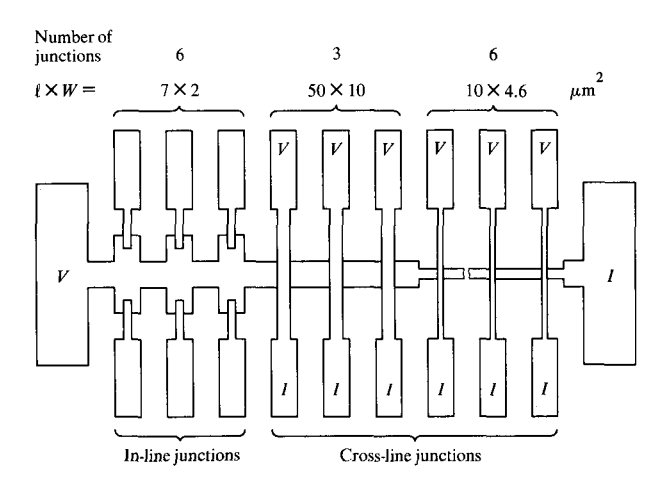


Figure 3 The junction test pattern used for measurement of electrical characteristics.

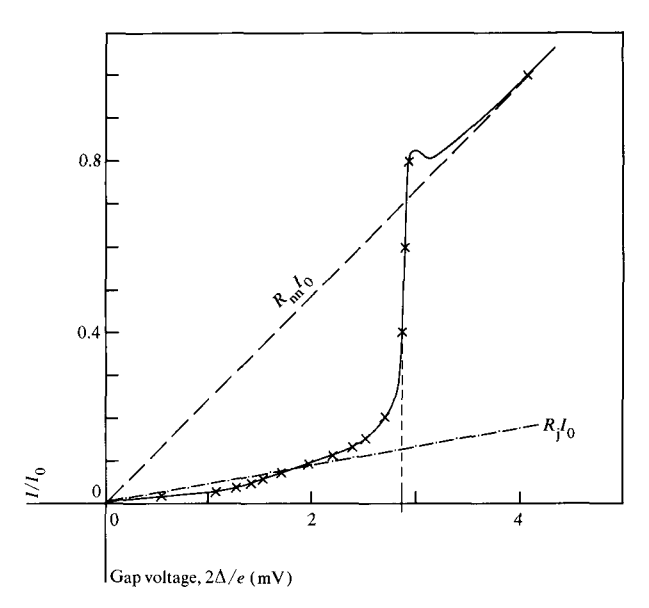


Figure 4 Plot of a typical I-V characteristic obtained with the automated system. The recorded points are indicated by the crosses. The ordinate is normalized to I_0 , the junction current at 4 mV.

Reproducibility from run to run was within $\pm 5\%$. Ellipsometer data from oxidized Nb surfaces were taken in the time span between 0.25 and 15 min of rf-plasma oxidation. The index of refraction finally reached for the niobium oxide was $2.75 \pm 1\%$ ($\kappa = 0$), independent of the Ar/O ratio and consistent with published data for thermally grown [37] and dc-plasma-anodized [38] films. Thinner oxide films usually had a larger n.

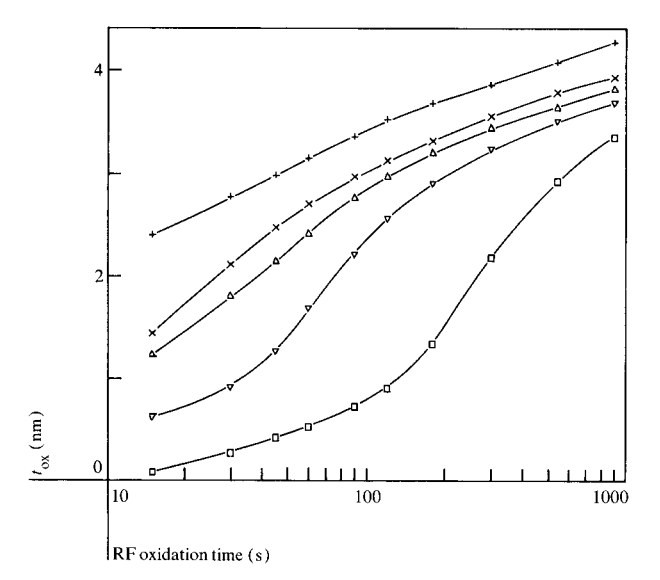


Figure 5 Results of ellipsometric measurements of oxide thickness *versus* rf oxidation time; the curves were obtained with O_2/Ar ratios of 33 (+), 4 (×), 2 (\triangle), 1 (∇), and 0.5 vol% (\square).

The dependence of oxide thickness t_{ox} on oxidation time for varying amounts of oxygen in the plasma is shown in Fig. 5. The slowest oxide growth occurs, as expected, at the lowest oxygen content. The oxidation time at 0.5 vol\% oxygen is long enough to permit thickness measurements of the first few monolayers. The initial slope of the growth curve is quite different from the region starting at about $t_{\rm ox} \ge 1$ nm. The slope changes again between $3.0 \le t_{\rm ox} \le 3.5$ nm, illustrating the nonuniform character of the oxidation mechanism where at least two parameters limit the rate of oxide growth. A detailed explanation is not available at present; however, the growth mechanism is believed to be complex because of the rf plasma that interacts electrochemically and mechanically with the surface of the Nb film and the as-grown oxide layer. This might be one reason why the logarithmic growth law observed for initial growth (≤0.8 nm) of tantalum-oxide films [39] is not generally found in our experiments. The rf plasma definitely accelerates oxide growth. In this context it might be interesting to note that rf cleaning of the surface of the base electrode with Ar also influences the oxidation process. The higher the rf voltage during argon cleaning, the thicker the as-grown oxide film and the lower the current density of junctions oxidized under otherwise identical conditions. The difference in the growth curves between the rf-cleaned and as-deposited Nb films is basically a parallel shift towards larger thicknesses. This implies acceleration of oxide growth in the very early stage of oxidation and may be understood as a consequence of surface damage by ion bombardment.

In Fig. 5 there is no evidence for a thickness limit, as expected from competing processes of oxide growth and sputter etching. This might be a consequence of the low plasma voltage used in this experiment resulting in a negligible sputter-etching rate. However, even for plasma voltages up to 400 V with 1 vol% O, in Ar there was no indication of saturation of the oxide thickness. The growth process appears to dominate over sputter etching, resulting in an oxide thickness that increases steadily with time. As will be shown, sputter etching of niobium oxide in pure Ar starts below 300 V; thickness saturation might therefore still be obtainable for a lower O2 content in the plasma, especially if operated at a low total pressure. This, however, was not tried because of the difficulty of accurately defining the gas composition and the increasing influence of gas desorption from the chamber walls. The conclusion from our ellipsometric studies is that oxide-thickness saturation, where j_1 becomes independent of time, could not be achieved under well-controlled experimental conditions. This is in contrast to the results for Pb and Pb-alloy junctions [31]. The interesting thickness range for Nb tunnel junctions is 2.5-3.5 nm $(j_1 = 1)$ to 10^4 A/cm²; see Fig. 6). The Nb/NbO /Pb junctions (\square) have current densities that are an order of magnitude lower than those for identical as-grown oxide thicknesses (×) [40]. This reflects a strong interaction of the Nb counter-electrode material with the barrier layer for the all-Nb junctions and/or formation of lead oxide at the barrier-tocounter-electrode interface for the Nb/Pb junctions.

• Electrical characteristics

The junction characteristics are relatively insensitive to changes in the fabrication conditions of the electrodes (e.g., varying the base-electrode thickness between 80 and 200 nm, varying the deposition rate between 1 and 4 nm/s, substituting base electrodes deposited in another uhv system, or patterning by etching vs lift-off). These variations all had little influence on V_m in comparison to the values obtained from reference junctions prepared simultaneously with standard electrodes in the same oxidation run. In contrast, the rf-plasma treatment of the base electrode immediately before, during, and after formation of the tunnel barrier had a much more drastic effect on the electrical characteristics. The principal results are summarized in Fig. 7, which shows the successive improvements in the I-V characteristic following introduction of various processing steps. All curves are normalized to a tunnel resistance $R_{\rm nn}=1~\Omega.$ The characteristic of an "ideal" BCS tunnel junction is indicated by the dashed line. Formation of the tunnel barrier directly on the asdeposited base electrode, after development of the stencil for the counter electrode, gave junctions with widely varying characteristics, sometimes nearly linear with only a small indication of the gap voltage. Curve 1 represents

one of the best examples. The oxidation conditions used are given in Table 1. No pre- or post-cleaning processes were used for these junctions.

Except where noted, these conditions were used for all the junctions reported here. Introduction of the pre-cleaning Ar plasma stage (see Table 1) greatly improved the reproducibility of the characteristics (Curve 2 of Fig. 7). Since the main purpose of this step is to remove surface contamination, thermal oxides, and thin films of the underlying Nb by means of sputter etching, we expect some dependence of the tunnel characteristics on the energy of the bombarding ions, which in turn is determined by both the gas pressure and the rf voltage. The threshold energy for oxide removal at an Ar pressure of 1 Pa is ≈300 V. Variation of Ar pressure from 0.5-5 Pa at a constant voltage of 350 V showed a decrease in $V_{\rm m}$ with pressures ≥2.7 Pa. This is most likely caused by a reduction in the energy of the Ar ions through the decrease in mean free path and/or increased backscattering of material from the surrounding cathode surface. In both cases the Josephson current density j_1 , for constant oxidation conditions, decreased with increasing ion energy (increasing voltage or decreasing pressure). Thus, the cleaned Nb surface must oxidize more rapidly with higher-energy Ar ion bombardment, indicating possible surface damage.

After oxidation of the tunnel barrier the rf discharge is terminated and the vacuum system is pumped down to $1-3\times 10^{-6}$ Pa. The adsorbed residual gases are removed (or another gas species is substituted) by a light plasma etch after formation of the barrier (see Table 1). This step improves the characteristics, as shown by Curve 3 in Fig. 7. A further improvement results when Ar is replaced with N_2 (see Table 1); the quasi-particle current at voltages $<2\Delta/e$ is reduced (Curve 4) and there is a marked increase in the dc Josephson current i_1 [see the shaded bands marked on Fig. 7; $i_1(4)$ corresponds to i_1 for Curve 4 conditions, etc.] although the value is still well below the theoretical maximum, $i_1(BCS)$.

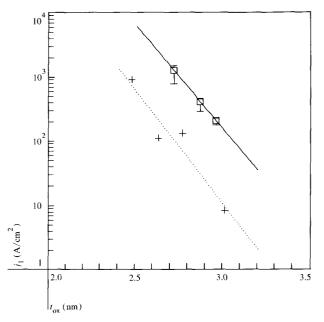


Figure 6 Josephson current density j_1 versus ellipsometrically determined oxide thickness for all-Nb junctions (\square), in comparison with data for Nb/NbO_x/Pb junctions (+) obtained from [40].

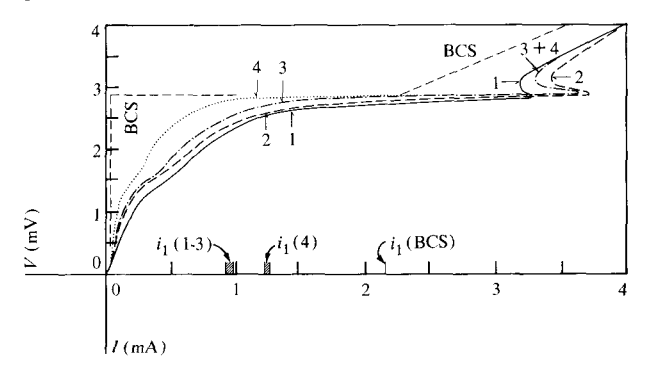


Figure 7 The influence of various processing steps on the I-V characteristics of Nb tunnel junctions. The conditions yielding Curves 1-4 are described in the text. Also shown is the "ideal" BCS quasi-particle characteristic (---) calculated for $\Delta/e = 1.42$ mV and T = 4.2 K. All curves are for $R_{\rm nn} = 1$ Ω . The value of i_1 obtained for Curve 4 conditions is shown as $i_1(4)$, that for the ideal BCS case as $i_1(BCS)$, etc.

Table 1 Optimal rf plasma conditions for preparation of tunnel barriers.

Process	Gas	Time (min)	Pressure (Pa)	$\begin{pmatrix} V_{\mathrm{r}^{\mathrm{f}}} \\ (\mathrm{V}) \end{pmatrix}$	Range of	
					$V_{\rm m}({ m V})$	$\frac{j_1(\text{measured})}{j_1(\text{BCS})}$
Pre-cleaning	Ar	15	1	340-400	3.0-3.5	$0.45 \pm 10\%$
Oxidation	$Ar + O_{a}$	1-2	5	140-160	_	_
Post-cleaning	Ar	12	10	140	4.0-4.5 ^a	$0.47 \pm 10\%$
Post-cleaning	N_{2}	12	10	190	$6.0-8.0^{a}$	$0.60 \pm 10\%$

[&]quot;Includes pre-cleaning

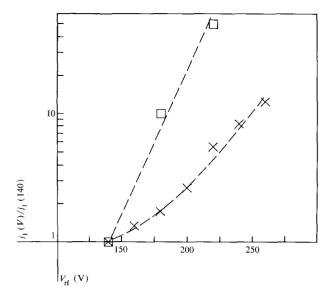


Figure 8 Influence of rf post-treatment voltage on j_1 normalized to $j_1(140)$, the value of j_1 for $V_{\rm rf}=140$ V. Time and gas pressure are 12 min and 10 Pa, respectively; Ar (\Box) and N_2 (\times) .

The dependence of j_1 on the rf voltage V_{rf} used for posttreatment is shown in Fig. 8. The ordinate is normalized to the value of j_1 at a post-treatment voltage of 140 V. Little change in j_1 occurs for $V_{\rm rf} \leq 140$ V for both Ar and N₂; Ar yields a much steeper dependence than N₂. Above 140 V, however, there is a tenfold increase in i_1 , corresponding to about a monolayer change in barrier thickness. Data from subgap tunnel currents (excess currents) for Nb/NbO ,/Nb and Nb/NbO ,/Pb junctions suggest that the upper interface between metal and oxide is mainly responsible for the higher quasi-particle currents of the former [7, 29]. Thus it appears that the interaction of the Nb atoms from the counter electrode with weakly bound oxygen atoms at the oxide surface is responsible for this degradation of the all-Nb I-V characteristics. This interaction could consist of the formation of lower (more conductive) oxides of Nb at the top interface. The improved characteristics with the Ar post-treatment appear to be the result of removing these weakly bound oxygen atoms from the surface just prior to the Nb evaporation. The increased j_1 for the Ar post-treatment may be due to a similar mechanism, i.e., removal of adsorbed oxygen from the oxide surface.

In the case of N_2 the effect is somewhat harder to clarify because N_2 can react both with the oxide, causing a reduction in the oxygen concentration at the surface, and with the Nb counter electrode, causing formation of NbN_x. Pure NbN is a superconductor with $T_c \approx 15 \text{ K}$ [41, 42]. Thus, the presence of nitrogen in the counter electrode may assist in counteracting degradation of T_c by

small amounts of oxygen present via interaction with the oxide. In the absence of supporting data from surface analysis, such as AES or ESCA, the explanations given here are speculative.

The optimum conditions (highest $V_{\rm m}$) listed in Table 1 were arrived at after numerous experiments in which pressure, rf voltage, and time were individually varied while all other parameters were fixed. The range of values obtained for the various processes are also listed in Table 1. No significant improvement was found on increasing the post-cleaning voltage above 200 V, or on reducing the pressure, suggesting that actual removal of the oxide (as opposed to removal of adsorbed atoms) does not improve the characteristics. Because of the rapid increase in j_1 with post-cleaning voltage (Fig. 8) it seems preferable to use the minimum voltage for control of the final current density j_1 .

For both Nb/NbO $_x$ /Nb and Nb/NbO $_x$ /Pb junctions (Ar pre-cleaned, no post-treatment) the quality ($V_{\rm m}$) decreased for rf-plasma voltages greater than 200-250 V. In contrast, the Josephson current density showed a strong dependence on oxidation time and the Ar/O $_2$ gas ratio (see Fig. 9). The $\log j_1$ decreased with increasing rf voltage at a pressure of 5 Pa for an Ar/O $_2$ ratio of 0.5 vol% and a constant oxidation time of 45 s. The value of $\log j_1$ is plotted against the independent variables to facilitate a comparison with the oxide thickness $t_{\rm ox}$. The current density j_1 is proportional to the tunneling conductance $G_{\rm nn}$, which in turn depends on $t_{\rm ox}$:

$$G_{\rm nn} \propto (-\alpha t_{\rm ox}),$$

where α is a function of barrier height and tunneling effective mass [43]. For small changes in $t_{\rm ox}$ it is reasonable to assume that α is constant; hence, $\log j_1 \propto t_{\rm ox}$. It can be seen that $t_{\rm ox}$ depends fairly linearly on log (oxidation time) and on $V_{\rm rf}$, within the range investigated. Because of the small oxide thickness range (2.5-3.5 nm), these results, and in particular the absence of saturation in oxide thickness with time, are consistent with the ellipsometric measurements described previously.

For many applications the stability of junctions at elevated temperatures (annealing), under extended storage at room temperature, and during thermal cycling between room temperatures and 4 K is of considerable importance. Annealing is necessary for more complex structures or processing requirements. Heat treatment of junctions at 80°C in pure N_2 led to an increase in j_1 and a small change in V_m . The average fractional change in j_1 , $j_1(t)/j_1(0)$, for a group of six $10 \times 4.6 \ \mu m^2$ junctions as a function of (annealing time t)^{1/2}, varied linearly from 1 to 1.5, indicating that the change in j_1 arises from a diffusion

process within the barrier. The increase in j_1 further suggests that the effective oxide thickness is reduced, possibly by out-diffusion of oxygen into the electrodes. This supposition is supported by the observation that any changes in $V_{\rm m}$ are usually towards lower values (about $-0.5~{\rm mV}$). Such changes are to be expected if the superconductor-oxide interfaces become more gradual. Annealing at temperatures above $100^{\circ}{\rm C}$ caused a more rapid deterioration in quality, and at $160^{\circ}{\rm C}$ many junctions short-circuited. Samples annealed for 40 h showed annealing factors of about 2.15 with a 35% reduction in $V_{\rm m}$.

Table 2 lists some results on the fractional change in Josephson current density after various periods of storage in dry air (desiccator) at room temperature (20-24°C). With two exceptions (array structures) the junctions were all of the type sketched in Fig. 3; they were not encapsulated by any surface coating and not annealed before the initial measurement determining $j_1(0)$. Junctions having post-treatment in N, rather than Ar show the larger ratios $j_1(t)/j_1(0)$, despite the longer storage times for the latter. The array structure junctions (to be discussed later) were covered by an evaporated film of SiO and control lines, and were annealed before the initial measurement. For these junctions the ratios $j_i(t)/j_i(0)$ are much smaller. In view of the linear dependence of this ratio on the square root of the annealing time, it is evident that a large part of the change in the "unannealed" junctions arises simply from "annealing" at room temperature. Thus, junctions can be stabilized by annealing.

●Interferometer arrays

Josephson junction interferometers [44] have been proposed as memory devices to store information as a single flux quantum $\Phi_0 = h/2e$ [45, 46]. Details and experimental results obtained with Pb-alloy junctions have been described by Guéret, Mohr, and Wolf [47]. They concluded from computer simulations that large arrays of singleflux-quantum (SFQ) memory cells could be realized, provided the necessary tolerances in the design parameters could be attained in practice. Of special interest is the operation of such memory cells in an array environment and, from a technological viewpoint, the variation in Josephson currents i, among the interferometers of the array. Experimental data on both these aspects are necessary to determine whether or not acceptable operating margins are possible. For these preliminary investigations, arrays of 80 interferometers have been designed and fabricated. The details have already been described for Pb-alloy junctions [48].

The absence of separate connections to every interferometer in the test pattern used (see Fig. 10) necessitated measurement only of the maximum dc Josephson

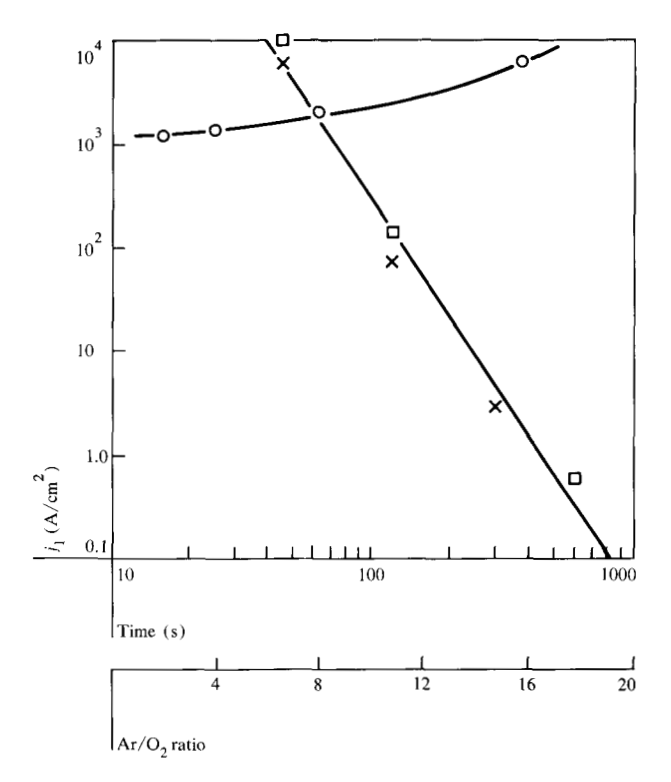


Figure 9 (a) Josephson current density j_1 versus rf oxidation time for O_2/Ar ratio of 12.5 vol%, $V_{rf} = 100 \text{ V}$ (×); and for O_2/Ar ratio of 4 vol%, $V_{rf} = 130 \text{ V}$ (\square). The pressure was $\approx 5 \text{ Pa}$. (b) Josephson current density versus the Ar/O_2 ratio for $V_{rf} = 100 \text{ V}$, oxidation time = 45 s, and pressure $\approx 5 \text{ Pa}$.

Table 2 Results on wafer storage at room temperature. Average values for $10 \times 4.6 \ \mu\text{m}^2$ and $50 \times 10 \ \mu\text{m}^2$ junctions, 6-9 junctions per wafer; no annealing unless indicated otherwise.

Post-treatment		Storage time t (days)	$j_1(t)$
Ar	N_2	(uuy 0)	$j_{1}(0)$
		124	1.30
		151	1.37
	▶	174	1.44
	✓	350 ^a	1.11 ^a
	1	400 ^a	1.04 ^a
1		619	1.22
1		700	1.27

^aAnnealed at 80°C 50 min, array structures of 80 two-junction interferometers

current i_1 , although in principle V_m can also be obtained. Selected chips (eliminating those with poorly defined films or other obvious defects) were measured. The mean current densities for some 13 wafers, with a total of 200 measured chips, ranged from 0.93-3.89 kA/cm² and 83% of the chips had a standard deviation σ in the Josephson current density of less than 2%. It is of particular interest

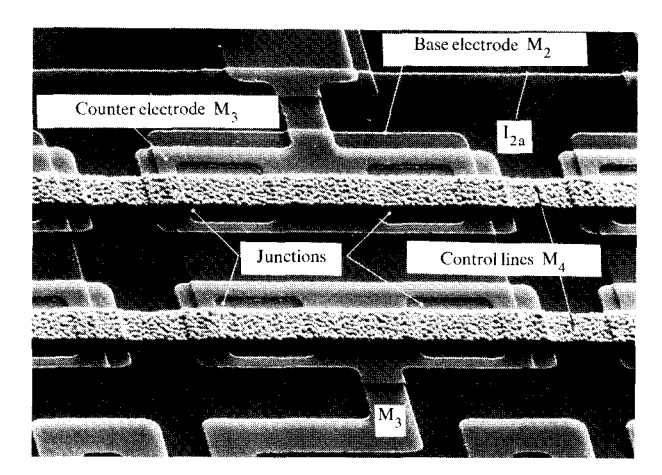


Figure 10 Projection of the Josephson currents of twelve 80-interferometer arrays. The values for a given array are normalized to its mean value of i_1 .

to note that in the selection process no defective junction was found among the interferometers. In almost all the cases exceptionally good reproducibility of i_1 within the arrays is obtained and σ is less than the maximum allowable value for a large SFQ array and also considerably lower than the values generally achieved with Pb-alloy junctions [48].

Several investigations into the effects of thermal cycling have been performed with encouraging results. Simple junctions and interferometer arrays have been cycled between room temperature and 4 K for 457 and 527 cycles. None of the devices were defective after these tests. It is also noteworthy that no insulation failures were observed between any of the films. The maximum spread of i_1 on the chips was within $\pm 6\%$ and the maximum change in i, after cycling was generally not greater than 1%. Some chips were annealed before cycling was begun, for times ranging from 45-576 min, and for these chips the change in i_1 is very small. Chips that had no annealing other than that introduced by the photoprocessing showed larger changes in i_1 (1-9%). These changes were not caused by the cycling itself but were most likely the result of some room-temperature "annealing" during storage after the first measurement. The absence of any cycling-induced defects indicates a failure probability per junction per cycle of less than 6×10^{-7} .

Summary

We have described the fabrication of thin-film Nb tunnel junctions using the techniques of e-beam evaporation and photoresist stenciling for making the electrodes, and oxidation in an rf plasma to form the tunnel barrier. The oxide formed by the plasma has been studied *in situ* by ellipsometry and indirectly by measurement of the tunneling characteristics after completion of the junctions. The ellipsometry measurements show that the oxide growth rate has a complex dependence on oxidation time, implying more than one mechanism. Unlike the plasma oxidation of Pb alloys [31], the Nb oxide growth rate has not been found to reach a saturation thickness with time within the range of parameters studied.

The junction I-V characteristic was found to depend rather critically on the processes used to form the tunnel oxide. In particular, pre-cleaning of the Nb surface in an Ar plasma with sufficiently energetic ions to remove thermal oxides by sputter etching is essential to obtain reproducible junction resistance and tunnel characteristics. A further new process, carried out after growth of the oxide (post-treatment), yielded a significant improvement. The post-treatment consisted in exposing the newly grown oxide to a low-voltage ($\leq 200 \text{ V}$), high-pressure ($\approx 1 \text{ Pa}$) plasma of either Ar or N₂. For both gases, the tunnel current at voltages below the gap voltage was reduced compared with untreated junctions. We believe the improvement was due primarily to the removal of adsorbed oxygen atoms on the surface of the oxide. Nitrogen was found to be more effective than Ar for post-treatment; not only was the reduction in the subgap quasi-particle current greater, but the dc Josephson current i, was also increased in comparison to those obtained for Ar-treated or untreated junctions. In this case, it is most likely that some N₂ is incorporated by substitution or inclusion in the surface of the oxide, where it may reduce the interaction of the Nb counter electrode with oxygen and decrease the thickness of the transition region between the tunnel barrier and the counter electrode. Furthermore, compared with O₂ treatment, the reaction of a small fraction of N, with the Nb should result in less degradation of the superconducting properties of the counter electrode, particularly in the neighborhood of the interface. Our comparative studies of junctions fabricated using all-Nb and Nb base electrodes with a Pb or Pb-alloy counter electrode [7, 49] also indicate that the interface between the tunnel barrier and the top electrode is important for obtaining high-quality junctions.

The junction quality was relatively insensitive to the conditions of the actual oxidation stage, provided the rf voltage was not too high (<200 V). In contrast, the Josephson current density j_1 was strongly dependent on time, rf voltage, and the Ar/O_2 ratio. As with the ellipsometer measurements, there was no evidence of a saturation in oxide thickness with increasing oxidation time. Within the small thickness range covered by the electrical

measurements, the oxide thickness $t_{\rm ox}$ was proportional to the logarithm of the oxidation time, and to the plasma voltage at fixed pressure and Ar/O₂ ratio.

Studies on the annealing of junctions at 80°C showed an increase in j_1 with time, roughly following a square root dependence. There was also a slight decrease in the junction quality, expressed by V_{m} . A possible explanation consistent with these observations is out-diffusion of oxygen from the oxide into the electrodes. Junctions that have been annealed and covered by a protective coating show very little change in their characteristics after long periods of storage at room temperature; changes in j_1 as low as 4.3% have been recorded after one year.

Thermal cycling between room temperature and 4 K was carried out on both simple unprotected junctions and on more complex arrays of 80 interferometers. None of the total of 1600 junctions failed after up to 527 cycles, nor did the characteristics change measurably except for a slight increase in j_1 .

Fabrication and electrical measurement of arrays of 80 two-junction interferometers were carried out as part of a preliminary investigation into the suitability of such devices for storage elements for cryogenic computers [45-47]. Of particular interest were the fabrication problems associated with the densely packed structure and the variations in the Josephson currents of the interferometers within the arrays. Fine structures with linewidths of 5 μ m could be successfully made with Nb. Recent work [50] using e-beam lithography has shown that 1-\mu structures and $1 \times 1-\mu m^2$ Josephson tunnel junctions can also be fabricated using Nb thin films. The standard deviation σ in i, within the arrays was in most cases less than 2% and in some cases less than 1%. These findings, together with the good stability of the junctions, are highly encouraging for the future design of working memory arrays having many thousands of cells.

Acknowledgments

We are most grateful to H. P. Gschwind, H. Richard, and H. Weibel for their assistance in making some of the electrical measurements. Thanks are also due H. Dietrich, W. Heuberger, and L. Perriard for their contributions to the preparation of the interferometer arrays.

References and note

- 1. J. Matisoo, IEEE Trans. Magnetics MAG-5, 848 (1969).
- 2. W. Anacker, IEEE Trans. Magnetics MAG-5, 968 (1969).
- H. H. Farrell and M. Strongin, Surface Sci. 38, 18 (1973); H. H. Farrell, H. S. Isaacs, and M. Strongin, Surface Sci. 38, 31 (1973).
- 4. I. Lindau and W. E. Spicer, Appl. Phys. 45, 3720 (1974).
- 5. M. Strongin and C. Varmazis, J. Appl. Phys. 46, 1401 (1975).

- 6. K. Schwidtal, J. Appl. Phys. 43, 202 (1972).
- R. F. Broom, R. Jaggi, R. B. Laibowitz, Th. O. Mohr, and W. Walter, in *Proceedings of the 14th International Confer*ence on Low Temperature Physics (LT 14), M. Krusius and M. Vuorio, Eds., North-Holland Publishing Co., Amsterdam, 1975, vol. 4, p. 172.
- 8. D. Sherrill and H. H. Edwards, *Phys. Rev. Lett.* 6, 460 (1961).
- 9. P. Townsend and J. Sutton, Proc. Phys. Soc. 78, 309 (1961).
- 10. P. Townsend and J. Sutton, Phys. Rev. 128, 591 (1962).
- M. H. Frommer, J. Bostock, K. Agyeman, R. M. Rose, and M. L. A. McVicar, J. Appl. Phys. 44, 5567 (1973).
- I. Giaever, in Proceedings of the 8th International Conference on Low Temperature Physics (LT 8), R. O. Davies, Ed., Butterworths, London, 1963, p. 171.
- 13. J. E. Nordman, J. Appl. Phys. 40, 2111 (1969).
- 14. L. O. Mullen and D. B. Sullivan, J. Appl. Phys. 40, 2115 (1969)
- 15. J. E. Nordman and W. H. Keller, Phys. Lett. A 36, 52 (1971).
- L. Y. L. Shen, in Superconductivity in d- and f-band Metals,
 D. H. Douglass, Ed., American Institute of Physics, New York, 1972, p. 31.
- L. S. Hoel, W. H. Keller, J. E. Nordman, and A. C. Scott, Solid-State Electron. 15, 1167 (1972).
- W. H. Keller and J. E. Nordman, J. Appl. Phys. 44, 4732 (1973).
- P. Rissman and T. Palholmen, Solid-State Electron. 17, 611 (1974).
- G. Paterno, P. Rissman, and R. Vaglio, J. Appl. Phys. 46, 1419 (1975).
- M. L. A. McVicar and R. M. Rose, Phys. Lett. A 25, 681 (1967).
- M. L. A. McVicar and R. M. Rose, J. Appl. Phys. 39, 1721 (1968).
- 23. M. L. A. McVicar and R. M. Rose, *Phys. Lett. A* 26, 510 (1968)
- R. B. Laibowitz and J. J. Cuomo, J. Appl. Phys. 41, 2748 (1970).
- 25. D. Bonnet and H. Rabenhorst, Phys. Lett. A 26, 174 (1968).
- D. Bonnet, S. Erlenkämper, H. Germer, and H. Rabenhorst, Phys. Lett. A 25, 452 (1967).
- R. B. Laibowitz and A. F. Mayadas, Appl. Phys. Lett. 20, 254 (1972).
- 28. G. Hawkins and J. Clarke, J. Appl. Phys. 47, 1616 (1976).
- 29. R. F. Broom, J. Appl. Phys. 47, 5432 (1976).
- ®AZ is a registered trademark of the Azoplate Division of American Hoechst Corporation, Somerville, NJ 08876.
- 31. J. H. Greiner, J. Appl. Phys. 42, 5151 (1971).
- Frank L. McCrackin, Tech. Note 479, National Bureau of Standards, Washington, DC, 1969.
- A. A. Guido, H. Cole, and L. B. Kriegbaum, *Proc. IEEE* 63, 1509 (1975).
- J. Matisoo, in Superconducting Machines and Devices, S. Foner and B. B. Schwartz, Eds., Plenum Press, New York, 1974, p. 563.
- V. Ambegaokar and A. Baratoff, Phys. Rev. Lett. 10, 486 (1963).
- W. L. McMillan and J. M. Rowell, in Superconductivity, R. D. Parks, Ed., Marcel Dekker and Co., New York, 1961, vol. 1, p. 561.
- J. J. Bellina, R. J. Lederich, and J. O'Neel, J. Appl. Phys. 43, 287 (1972).
- 38. K. Knorr and J. D. Leslie, J. Electrochem. Soc. 121, 805 (1974)
- 39. P. B. Sewell, D. F. Mitchell, and M. Cohen, Surface Sci. 29, 173 (1972).
- S. Basavaiah and J. H. Greiner, J. Appl. Phys. 47, 4201 (1976).
- 41. G. V. Samsonov and V. S. Nesphor, Sov. Phys. JETP 3, 947 (1957).
- 42. A. Aubert and J. Spitz, Le Vide 175, 1 (1975).
- 43. J. G. Simmons, J. Appl. Phys. 34, 1793 (1963).

- T. A. Fulton, L. N. Dunkelberger, and R. C. Dynes, *Phys. Rev. B* 6, 855 (1972).
- 45. H. H. Zappe, Appl. Phys. Lett. 25, 424 (1970).
- 46. P. Guéret, Appl. Phys. Lett. 25, 426 (1970).
- 47. P. Guéret, Th. O. Mohr, and P. Wolf, IEEE Trans. Magnetics MAG-13, 52 (1977).
- Th. O. Mohr and R. F. Broom, J. Vac. Sci. Technol. 15, 1166 (1978).
- 49. R. F. Broom, J. Appl. Phys. 47, 5432 (1976).
- R. Voss, R. Laibowitz, S. I. Raider, W. D. Grobman, and J. Clark, Bull. Amer. Phys. Soc. 24, 264 (1979).

Received March 16, 1979; revised August 30, 1979

R. F. Broom, Th. O. Mohr, and W. Walter are located at the IBM Zurich Research Laboratory, 8803 Rüschlikon, Switzerland. R. B. Laibowitz is located at the IBM Thomas J. Watson Research Center, Yorktown Heights, New York 10598.